REPORT DOCUMENTATION PAGE

Form Approved
OMB No. 0704-0188

2. REPORT DATE	3. REPORT TYPE AND DATES COVERED
c. 12, 1990	Final 9/20/89 - 9/19/90

4. TITLE AND SUBTITLE

Molecular Dynamics Simulator for Optimal Control of Molecular Motion

5. FUNDING NUMBERS

DAAL03-89-K-0173

6. AUTHOR(S)

Herschel Rabitz

7. PERFORMING ORGANIZATION NAME(S) AND ADDRESS(ES)

Department of Chemistry
Princeton University
Princeton, NJ 08544-1009

8. PERFORMING ORGANIZATION REPORT NUMBER

9. SPONSORING/MONITORING AGENCY NAME(S) AND ADDRESS(ES)

U. S. Army Research Office
P. O. Box 12211
Research Triangle Park, NC 27709-2211

10. SPONSORING/MONITORING AGENCY REPORT NUMBER

ARO 27577.1-CH

11. SUPPLEMENTARY NOTES

The view, opinions and/or findings contained in this report are those of the author(s) and should not be construed as an official Department of the Army position, policy, or decision, unless so designated by other documentation.

12a. DISTRIBUTION/AVAILABILITY STATEMENT

Approved for public release; distribution unlimited.

12b. DISTRIBUTION CODE

13. ABSTRACT *(Maximum 200 words)*

In recognition of recent interest in developing optimal control techniques for manipulating molecular motion, this paper introduces a computer-driven electro-mechanical analog of this process. The resultant Molecular Dynamics Simulator (MDS) is centered around a linear air track for which the atoms of the controlled molecule are simulated as nearly frictionless carts on the track. Bonds in the simulated molecule are described by precision springs, and the interaction with an external optical field is simulated through a computer-based linear driver. When the MDS is operated in the harmonic regime, it can be used as an exact analog of molecular scale quantum systems through Ehrenfest's Theorem, or equivalently as a classical set of coupled oscillators. The tools of optimal control theory currently being applied at the molecular scale are used to design the forcing function for the MDS. Optical encoders are used to measure bond distances for graphic representation of the MDS behavior. Bond breaking can also be simulated by bond-length sensitive trigger-release mechanisms. The MDS is especially useful as a modelling tool to bridge theoretical studies and eventual laboratory experiments at the true molecular scale

14. SUBJECT TERMS

MOLECULAR DYNAMICS, CONTROL THEORY

15. NUMBER OF PAGES

25

16. PRICE CODE

17. SECURITY CLASSIFICATION OF REPORT	18. SECURITY CLASSIFICATION OF THIS PAGE	19. SECURITY CLASSIFICATION OF ABSTRACT	20. LIMITATION OF ABSTRACT
UNCLASSIFIED	UNCLASSIFIED	UNCLASSIFIED	UL

MOLECULAR DYNAMICS SIMULATOR FOR OPTIMAL CONTROL OF MOLECULAR MOTION

Final Report

by

Herschel Rabitz

December, 1990

U.S. Army Research Office
Grant #DAAL03-89-K-0173

Department of Chemistry
Princeton University

I. INTRODUCTION

Controlling molecular motion with laser fields has been a long sought-after goal without much demonstrated success. Most earlier work relied on what was thought to be sound physical intuition to "design" optical fields for the purpose of effective bond breaking, or otherwise selectively manipulating molecular motion. Theoretical studies have shown that such approaches are not well founded given the complexities of molecular motion. It is evident that a more systematic design process is needed. The method of optimal control theory is one such systematic approach used in the treatment of complex classical engineering systems, and, most recently, such methods have been considered for the design of optical fields to meet specific molecular objectives[1,2].

The introduction of optimal control theory at the molecular scale is an on-going development with many interesting aspects and attributes. In particular, this approach is capable of establishing the existence and identifying the type of external forcing functions necessary to control the motion of any particular molecule. The purpose of the theory, ultimately, is to produce reliable designs of optical fields that are practical to apply to molecular samples in the laboratory. Current developments of optical pulse shaping in the ultrafast regime (< 1 ps) are expected to be an integral part of such laboratory studies. The latter tools are hardly routine at this stage of development and, given the previous frustrating experimental studies, it is appropriate to seek an intermediate bridge between the theory and ultimate experiments. The Molecular Dynamics Simulator (MDS) reported in this paper was explicitly constructed for the purpose of filling this gap. The simulator is an analog in the sense that its dynamics can be made to satisfy exactly the same equations of motion as those at the molecular scale under appropriate circumstances. For example, in the case of harmonic molecular motion, Ehrenfest's Theorem prescribes that the expectation value of the atomic positions will satisfy the corresponding equations of classical mechanics. Similarly, achieving designs of optimal controlling fields for even moderate size polyatomic molecules will necessitate the use of classical mechanics and, once again, a

benchtop simulator will have the same physics. The principal difference between the analog and the real molecular system entails a change of time scale to translate the ultrafast phenomena at the molecular scale to phenomena observable in a slowly oscillating mechanical system at the macroscopic scale.

The potential role of an MDS as a research tool as well as a pedagogical guide can be recognized by recalling the importance of ball-and-stick models of molecules and crystals as an aid to understanding molecular structure. The complexities of molecular dynamics go beyond that of structure, and an active flexible MDS should play a valuable role in providing insight for controlling molecular motion using external fields. The MDS introduced in this paper should be viewed as an initial version with various additional levels of sophistication capable of being introduced for enhanced utility.

Section II will describe the underlying physics behind the MDS and give a brief summary of the optimal control techniques used to design the external forcing function. Section III will describe the actual make-up of the MDS and its general characteristics. Illustrations of the behavior of the MDS will be given in Section IV with a brief conclusion given in Section V.

II. THEORY

We review here the equations of motion for carts connected by springs on an almost frictionless air track driven on one end by a linear motor in analogy with an optically forced linear molecule. A cost functional is introduced which, when minimized, will yield a driving function to manipulate the carts in a desired manner. The Hamiltonian for the nuclear degrees of freedom of a molecule modelled as a harmonic oscillator in the presence of an external field $\varepsilon(t)$ coupled to a linear dipole can be written as:

$$H = 1/2\ p^T Gp + 1/2\ q^T Fq - q^T b\ \varepsilon(t) \qquad (2.1)$$

where q is a vector containing displacements of internal coordinates from their equilibrium positions, p are the conjugate momenta, G is the Wilson G matrix[3] with units of inverse mass, F is the matrix of harmonic force constants, and b is the vector of dipole moment derivatives of the

molecule. The MDS can be extended to the anharmonic regime, but this initial work will be confined to the harmonic case.

Our molecular simulator consists of a number of carts representing atoms connected by springs taken as bonds. The assembly is constrained to move in one dimension by the air track and is driven at one end by a motor representing the laser-molecule interaction. See Figure 1.

The Hamiltonian for the MDS is identical to Equation (2.1) for all of the cases treated in this paper. The molecular masses, force constants, and dipole derivatives are simply replaced by parameters appropriate for the MDS. The effect of the springs having finite mass (less than 1% of a cart mass) was adequately treated by adding 1/2 of each spring mass to both adjacent carts.

The equations of motion for this system modified for the presence of friction are given by Hamilton's equations:

$$\dot{q} = \frac{\partial H}{\partial p} = Gp(t) \tag{2.2a}$$

$$\dot{p} = -\frac{\partial H}{\partial q} - \alpha p = -Fq + b\varepsilon(t) - \alpha p \tag{2.2b}$$

where the last term was added to compensate for friction which is not present as such in the dynamics of molecular systems. Here α is the coefficient of friction which was assumed to be the same for all carts. The equations of motion can be rewritten in a compact form as:

$$\dot{z}(t) = f[z(t),\varepsilon(t)] \tag{2.3}$$

where $z^T(t) = [q^T(t), p^T(t)]$, and is referred to as the state of the system. We assume that the initial state is known and corresponds to the system at rest, $z(0) = 0$. Note that the simulator coordinate system (displacement of carts) is different from the bond displacements which are natural molecular coordinates; this will be addressed later in this section.

Now, the goal is to design a driving function $\varepsilon(t)$ to achieve some target objective in the simulator while disturbing the rest of the system as little as possible. In addition, there is a mechanical limitation on the magnitude of $\varepsilon(t)$. In keeping with the molecular analogy, we choose our target to be selective excitation of one cart or bond. We define selective excitation as achieving a desired displacement of one cart or bond at a target time, T, while the displacements and momenta of the rest of the carts or bonds are as small as possible during the entire pumping interval $0 \leq t \leq T$.

To obtain a driving function which selectively excites the simulator, we introduce a cost functional

$$J = \Phi[z(T)] + \int_0^T L[z(t), \varepsilon(t)]\, dt \qquad (2.4)$$

where $\Phi[z(T)]$ is an error function for the state not reaching the target γ:

$$\Phi[z(T)] = 1/2\ [z(T) - \gamma]^T\ P_f\ [z(T) - \gamma] \qquad (2.5)$$

and P_f is a diagonal weighting matrix. The second term in Equation (2.4) seeks to minimize the energy in the molecule and that of the driving function over the control interval:

$$L = 1/2\ z^T(t)Wz(t) + 1/2\ w_e\ \varepsilon^2\ (t) \qquad (2.6)$$

where W is a diagonal matrix weighting displacement and momentum during the control interval, and w_e weights driver displacement. The weighting factors are adjusted until the driving function has an acceptable peak magnitude and the target is satisfactorily reached. The target displacements and momenta can alternatively be constrained to a target value instead of being included in the cost function where the target error function is balanced against other costs[2].

To include the equations of motion (2.3) in the minimization process, Lagrange multipliers are introduced in an augmented cost functional:

$$\bar{J} = J - \int_0^T dt\lambda^T(t)\ [\dot{z} - f(z,\varepsilon)] \tag{2.7}$$

Varying $\varepsilon(t)$ and $z(t)$ infinitesimally by $\delta\varepsilon(t)$ and $\delta z(t)$, respectively, produces the following change in the augmented cost functional:

$$\begin{aligned}\delta\bar{J} &= [z(T) - \gamma]^T P_f\ \delta z(T) \\ &+ \int_0^T dt[z^T W\delta z(t) + \omega_e\ \varepsilon(t)\ \delta\varepsilon(t)] \\ &- \int_0^T dt\lambda^T(t)\ [\delta\dot{z}(t) - \frac{\partial f}{\partial z}\ \delta z(t) - \frac{\partial f}{\partial \varepsilon}\ \delta\varepsilon(t)]\end{aligned} \tag{2.8}$$

Integrating by parts and rearranging, we obtain

$$\begin{aligned}\delta\bar{J} &= \{[z(T) - \gamma]^T P_f - \lambda^T(T)\}\ \delta z(T) \\ &+ \int_0^T dt[z^T W + \dot{\lambda}^T + \lambda^T \frac{\partial f}{\partial z}\ ]\ \delta z(t) \\ &+ \int_0^T dt[\omega_e\varepsilon(t) + \lambda^T \frac{\partial f}{\partial \varepsilon}\ ]\ \delta\varepsilon(t)\end{aligned} \tag{2.9}$$

If we choose

$$\dot{\lambda} = -Wz - \left(\frac{\partial f}{\partial z}\right)^T \lambda \tag{2.10}$$

with the final condition

$$\lambda(T) = P_f\ [z(T) - \gamma], \tag{2.11}$$

then the equation for the gradient of $\bar{J}$ with respect to the driving field becomes

$$\frac{\delta\bar{J}}{\delta\varepsilon(t)} = \omega_e\varepsilon(t) + \lambda^T(t)\ \frac{\partial f}{\partial \varepsilon} \tag{2.12}$$

This equation can be set to zero and, since the equations of motion are linear in the present case, $\varepsilon(t)$ can be solved for in analytical form.

The case we considered was a system of three carts connected by springs in the linear regime. The Hamiltonian for this case is explicitly:

$$H = 1/2\ p^T Gp + 1/2\ q^T Fq + k_1 q_1\ \varepsilon(t) \qquad (2.13)$$

where $G_{ij} = \delta_{ij} M_i^{-1}$, M_i is the mass of the i^{th} cart and $F_{ij} = \delta_{ij}\ (k_i + k_{i+1}) - \delta_{i(j-1)} k_{i+1} - \delta_{i(j+1)} k_i$ where k_i is the force constant of the i^{th} spring. Cart one is connected via spring one to the driving arm. Because this Hamiltonian yields linear equations of motion, it was possible to conveniently constrain the target coordinate to a desired value at $t = T$.

In order to specify a target which was the analog of a bond stretch, we transformed to the following coordinate system:

$$Q = Sq \qquad (2.14a)$$

where

$$S = \begin{pmatrix} 1 & -1 & 0 \\ 0 & 1 & -1 \\ 0 & 0 & 1 \end{pmatrix} \qquad (2.14b)$$

Q_1 is the displacement from equilibrium of the spring between carts one and two, Q_2 is the displacement of the spring between cart two and three, and Q_3 is the displacement of cart three from equilibrium. The momenta conjugate to Q are given by a point transformation[4]

$$P_i = \sum_j P_j \frac{\partial q_j}{\partial Q_i} \qquad (2.15)$$

or $P = (S^{-1})^T p$. The Hamiltonian can be rewritten as

$$H = 1/2\ P^T G'P + 1/2\ Q^T F'Q + k_1\ (Q_1 + Q_2 + Q_3)\ \varepsilon(t) \qquad (2.16)$$

where

$$F' = (S^{-1})^T FS^{-1} \tag{2.17}$$

$$G' = SGS^T \tag{2.18}$$

In this new coordinate system it is possible to specify objectives which correspond to bond stretches.

The internal nuclear motion of molecules is properly treated using quantum mechanics, but our simulator is described by classical mechanics. In the linear regime, the classical values of displacement and momenta are the same as the quantum expectation values of these quantities according to Ehrenfest's theorem. Classical mechanics is not equivalent to quantum mechanics in describing the dynamics of molecules with anharmonic potentials. Nevertheless, classical molecular simulations are necessary because quantum calculations are most often prohibitively difficult for even the fastest computers.

III. APPARATUS

The Molecular Dynamic Simulator (MDS) in this study models atoms in molecules as simple masses and interatomic forces as springs. Both linear and nonlinear springs are possible, although this version of the simulator considers only linear springs (Multi-Flex Corporation) with an example shown in Fig. 2. It can be seen that the springs are highly linear for stretches used in the simulator. The springs were of the extension type and were fully compressed when unloaded. The spring constants were in the range of 3000-3500 dynes/cm with each carefully measured statically. Although discrepancies can arise between the static and dynamic response of springs, the excellent results in Section IV indicate that this was not a problem here. The interaction of molecules with external optical fields is modelled by a mechanical linear driver that is used to couple energy to the simulated molecule through a spring connected to a mass at one end of the chain of simulated coupled atoms.

The masses of the simulated molecule are carts that float on a linear wedged air track as shown in Fig. 1. The position of each mass is monitored by an adjacent optical position detector (SiTek Corporation) that locates the centroid of a point light source (battery-operated light-emitting-diode) affixed to each cart. The optical position detectors have 11 bits of resolution over a length span of 1 or 3 cm depending on the diode array selected.

The driver that simulates the interaction with external optical fields is a speaker coil excited by a current source (PASCO Corporation). The current source has been modified to implement position feedback using a PID (Proportional Integral Derivative) controller. Feedback control was added to eliminate an undesirable dependency of the driver on the properties of the load. The use of feedback here effectively endows the driver with an infinite mass corresponding to the optical field not being significantly perturbed by the molecular sample. Note that this type of feedback does not alter the fact that the simulated molecule is being controlled in an open loop fashion. An example of a typical forcing function is shown in Fig. 3a. Both the designed forcing function and the measured forcing function are plotted in this figure.

The carts are each approximately 200 grams and are about 15 cm long. Given that the air track is 2 meters long, the largest molecule that was possible to simulate was a linear tri-atomic. A longer track could readily handle larger simulated polyatomic molecules. Damping of the carts on the air track was minimal, although non-negligible, exhibiting a decay constant α^{-1} of approximately two minutes.

A laboratory computer using the optical position sensors recorded the cart driver positions by means of a standard 12-bit resolution A/D-D/A interface. This computer also specified the desired forcer function.

Based on measurements of the cart masses, the stress-strain relationships of the springs, and cart damping constants, an optimal forcing function was computed for the achievement of a particular goal. The goal might be, for

example, the 2 cm stretching of the spring between carts 1 and 2 at T=30 seconds, subject to the minimization of the stretch between carts 2 and 3 over the interval $0 \leq t \leq 30$ seconds. The laboratory computer is used both to synthesize the driving function as well as to record the position of the driver and the carts. The computer sampling rate is nominally 40 Hz, which is greatly in excess of the characteristic oscillation frequency of the system, which is nominally 1 Hz. Because of this large difference, significant effects due to discretization of time are not expected.

To demonstrate bond breaking, a special spring is used involving a trip cord that releases the spring when a threshold length is reached. As will be discussed later, the use of this "breakable bond" graphically illustrates a goal that, if achieved at the molecular scale, would be most significant.

IV. RESULTS

The results presented here were produced using three carts on an air track with a spring between each cart and springs on either end, one end being fixed and the other connected to the driver arm as shown in Fig. 1.

As a first target, we chose to specify the displacement of the second cart to be 1.0 cm at a run time of T=30 seconds. The weights W and w_e in Eq. (2.7) were chosen such that the maximum amplitude of the driving function did not exceed the mechanical limit of the driver, which was about 0.34 cm. Figure 3 shows the resulting optimal driving function and the system response. Figure 3a shows the theoretical driving function and the actual experimental driver arm displacement to be nearly identical. It can be seen that the driving function is a complicated waveform and its power spectrum in Fig. 3b shows that it consists of all three modes of the system. Figures 3c and 3d show experimental and theoretical displacement for the first and second carts, respectively, and show that the carts accurately follow their predicted motion. The initial low amplitude portion of the driving function prepares the system to have the proper phase structure in order to receive the energy pumped in during the latter part of the driver pulse. Because the driver, due to its mechanical limit, cannot deliver enough energy to reach the target in a short pulse, it must slowly pump

energy into the simulator over a large portion of the control interval. This situation is analogous to working with an optical field of limited intensity. The energy remains delocalized among the carts and springs until close to the target time when it becomes localized or coalesces in the desired displacement of the second cart. The first cart's experimental peak amplitude is 0.66 cm, well below the observed value of the second cart at the final time of 0.96 cm. The displacement of the third cart is not observable using our experimental set-up, but the peak theoretical amplitude for this cart is 0.64 cm. This case succeeded in controlling the displacement of the second cart while keeping the motion of the other two carts to a minimum, and the driver as seen in Fig. 3a does not exceed its limit.

In Figs. 3c and 3d, one can see that at t=0, there was significant deviations of the system from its nominal initial condition of being at rest. However, it was noticed that the target was remarkably insensitive to this initial noise. A simple demonstration of this robustness to the initial state is shown as follows. The carts were started with arbitrary oscillation amplitude of about 0.2 cm at t=0, and again subjected to the driving function shown in Fig. 3a. The second cart reached 1.13 cm at the target time, about 13% different than the target value of 1.0 cm, and the peak amplitude of the first bond was 0.80 cm. This shows that, with initial oscillations of about 20% of the target displacement, the system dynamics were still acceptable and the target was reasonably achieved. A more formal robustness study should be performed to confirm this result, but it was our observation that the system was reasonably insensitive to initial conditions for many different cases. For linear systems, the sensitivity of the state at the final time to the initial conditions is quite simple. For nonlinear systems the relationship is more convoluted and a driving function which minimizes this sensitivity could be obtained if the sensitivity were included as another term in the cost function.

While in the previous case the coordinates controlled by the cost function were cart displacements, natural coordinates for specifying molecular objectives would include bond stretches and not atom displacements in the

laboratory reference frame. We used Equation (2.14) to transform to a coordinate system containing two bond stretches and a translation-like degree of freedom which does not get weighted in the cost function. The two springs between the three carts can be pictured as bonds, and now we will consider the case where the target is a bond stretch.

Figure 4 shows results for using a cost functional in which the first bond is constrained to reach 1.03 cm at T=30 seconds while the motion of the second bond and driver amplitude are minimized. Figure 4a shows the designed and measured forcing function for this case which consists, once again, of a combination of frequencies. It also begins with a small amplitude phase aligning period followed by heavy pumping near the target time. Figure 4b shows the experimental and theoretical displacement of the first bond. The good agreement between experiment and theory and the relative insensitivity of the final state to initial noise are seen once again. The experimental final stretch was 0.95 cm in comparison with the theoretical stretch of 1.03 cm. Figure 4c shows a comparison of the theoretical stretches of the two bonds. The peak stretch of the second bond was 0.91 cm at about 28 seconds, while the target bond reaches 1.03 cm at the end. These bond extensions correspond to the first bond exceeding its limit (breaking), while the second bond remained stretched below its limits. The displacement of the nontarget bond could be reduced further by changing the appropriate weighting factors in the cost functional (2.5).

The results for the interchanged case with the theoretical design constraining the second bond to be 1.03 cm at T=30 seconds, while minimizing the stretch of the first bond and the displacement of the driver, can be seen in Fig. 5 and shows the power of the optimal control method. The MDS configuration is simulating the same molecule as in Fig. 4, but the target bonds are now interchanged. Figure 5a shows the nontrivial driving field, and Fig. 5b shows the theoretical stretches of bond 1 and bond 2. It is seen that, while bond 2 stretches to 1.03 cm at the target time, the nontarget bond is never displaced by more than 0.75 cm from equilibrium.

Indeed, the experimental results in Fig. 5c show that the first bond never exceeds 0.90 cm during its excursion. This success shows that bond 2 "breaks" while bond 1 does not.

5. CONCLUSION

Given the current active interest in the area of controlling molecular motion, this paper presents a workable computer-controlled electro-mechanical MDS. The linear MDS with harmonic springs can already simulate realistic molecular scale events, but further extensions would be useful. In particular, a two-dimensional MDS using an air table rather than an air track would open up a wider variety of molecular examples for study. Even in the one-dimensional domain , the introduction of precision anharmonic springs to simulate more realistic bond stretching would be valuable. As the MDS is inherently a classical mechanical device, it can be used to explore the degree of control achievable in coupled classical anharmonic oscillator systems, including those displaying chaotic motion. In summary, at a rather modest expense and effort, it is possible to construct a practical MDS that is useful for both pedagogy and research.[5]

REFERENCES

1. S. Shi, A. Woody, and H. Rabitz, J. Chem. Phys 88, 6870 (1988).

   S. Shi and H. Rabitz, "Optimal Control of Bond Selectivity in Unimolecular Reactions," in press, J. Comp. Phys.

   R. Kosleff, S.A. Rice, P. Gaspard, S. Tersigni, and D.J. Darrst, Chem. Phys. 139, 201 (1989).

2. C. Schwieters, J.G.B. Beumee, and H. Rabitz, J. Opt. Soc. Am. B 7, 1736 (1990).

   J.G.B. Beumee and H Rabitz, "Application of Optimal Control Theory for Selective Vibrational Excitation in Molecules Modelled as Harmonic Physical Systems," (submitted to J. Math. Phys.).

   S.Shi and H. Rabitz, Chem. Phys. 139, 185 (1989).

3. E.B. Wilson, Jr., J.C. Decius, and P.C. Cross, Molecular Vibrations, McGraw-Hill (1955), p. 61.

4. H. Goldstein, Classical Mechanics, 2nd Edition, Addison-Wesley, (1980) p. 378.

5. This report forms the body of a manuscript authored by M. Husman, E. Schweiters, M. Littman and H. Rabitz, Am. J. Phys., submitted.

FIGURE CAPTIONS

Figure 1. Schematic of the Molecular Dynamics Simulator.

Figure 2. Measurement of force versus distance for four different linear springs. Each symbol represents a data point and a line was fit to each data set showing that the springs are quite linear in this region of interest.

Figure 3. Results for control of the 3-cart MDS where the objective is displacement of cart 2 to 1.0 cm at T = 30 seconds: (a) predicted (solid curve) and observed (points) driving field, (b) power spectrum of the driving field showing the presence of all three fundamental frequencies of the MDS, (c) response of cart 1, and (d) response of cart 2. It is seen that the carts follow the theoretical predictions quite well and that cart 2 has achieved its target at the final time.

Figure 4. Results for control of the 3-cart MDS where the objective is displacement of bond 1 to 1.03 cm at T = 30 seconds: (a) predicted (solid curve) and observed (points) driving field, (b) predicted and observed stretch of bond 1, and (c) comparison of theoretical stretches of bond 1 (solid curve) and bond 2 (dashed curve). Bond 1 achieves the "breaking distance" of 1.03 cm at the final time, while bond 2 remains below this threshold with a maximum stretch of 0.91 cm.

Figure 5. Results for control of the 3-cart MDS where the objective is displacement of bond 2 to 1.03 cm at T = 30 seconds: (a) predicted (solid curve) and observed (points) driving field (b) comparison of theoretical stretches of bond 1 (solid curve) and bond 2 (dashed curve), and (c) predicted and observed stretch of bond 1. Bond 2 achieves the "breaking distance" of 1 cm at the final time, while bond 1 remains below this threshold with a maximum stretch of 0.90 cm.

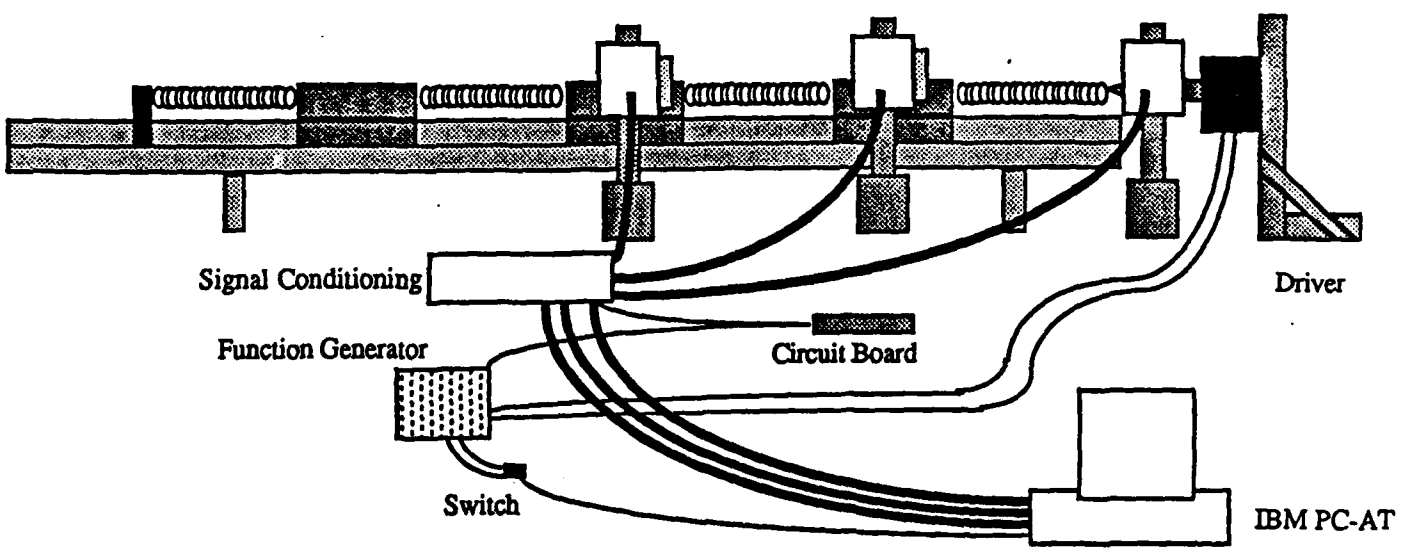
Signal Conditioning
Driver
Function Generator
Circuit Board
Switch
IBM PC-AT

Figure 1

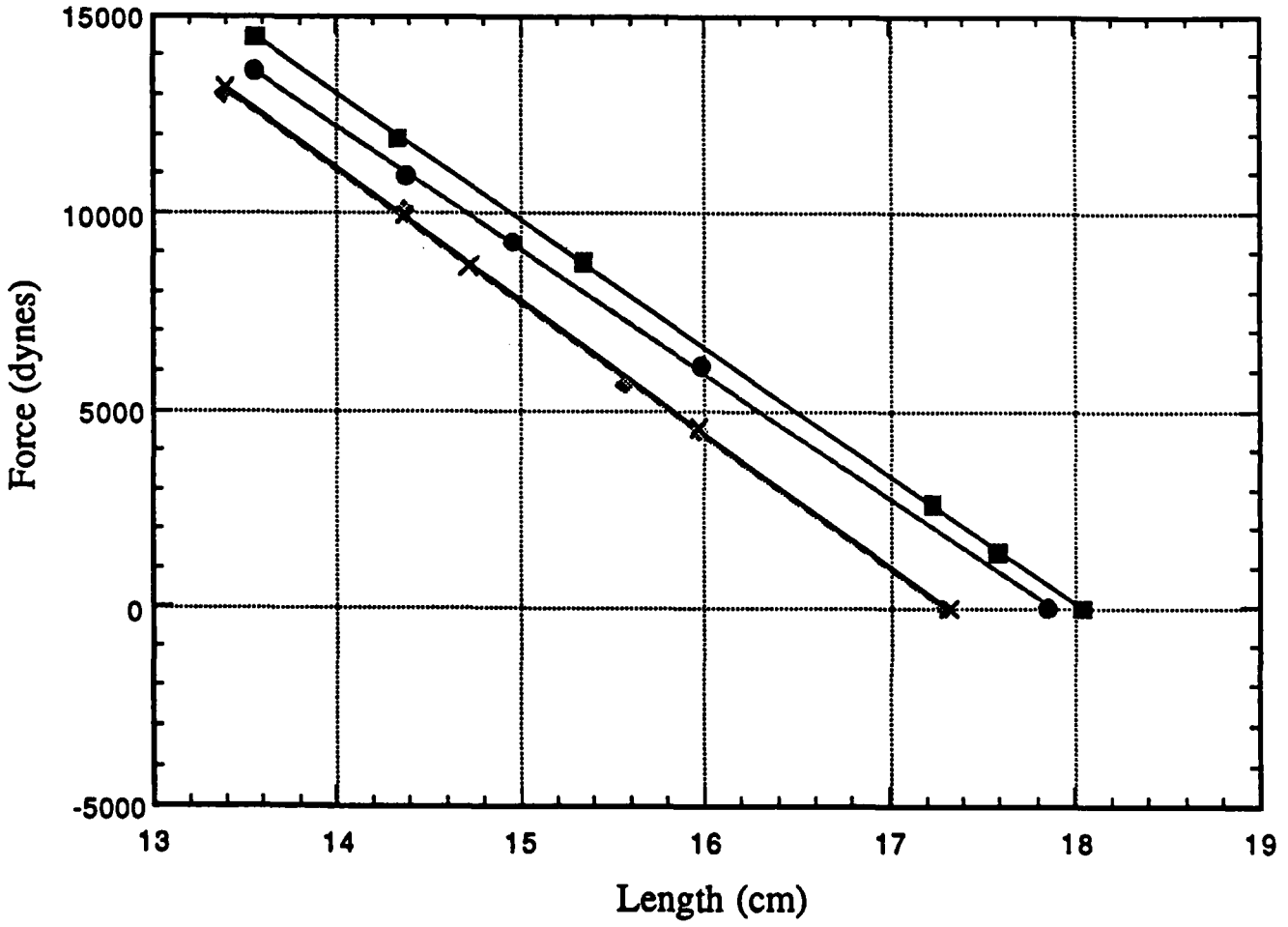
15000
10000
5000
0
-5000
Force (dynes)
13
14
15
16
17
18
19
Length (cm)

Figure 2

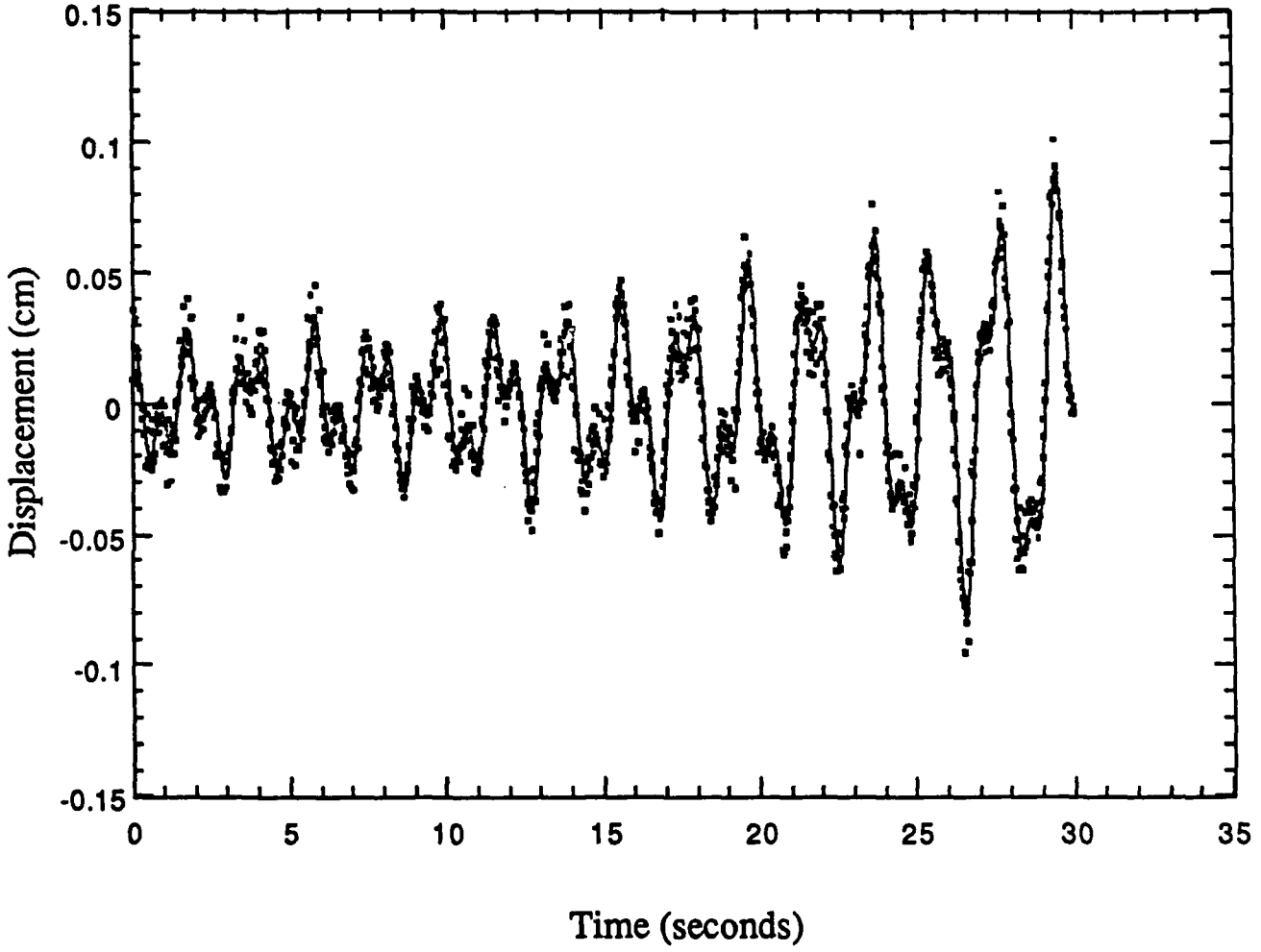
0.15
0.1
0.05
0
-0.05
-0.1
-0.15
Displacement (cm)
0
5
10
15
20
25
30
35
Time (seconds)

Figure 3a

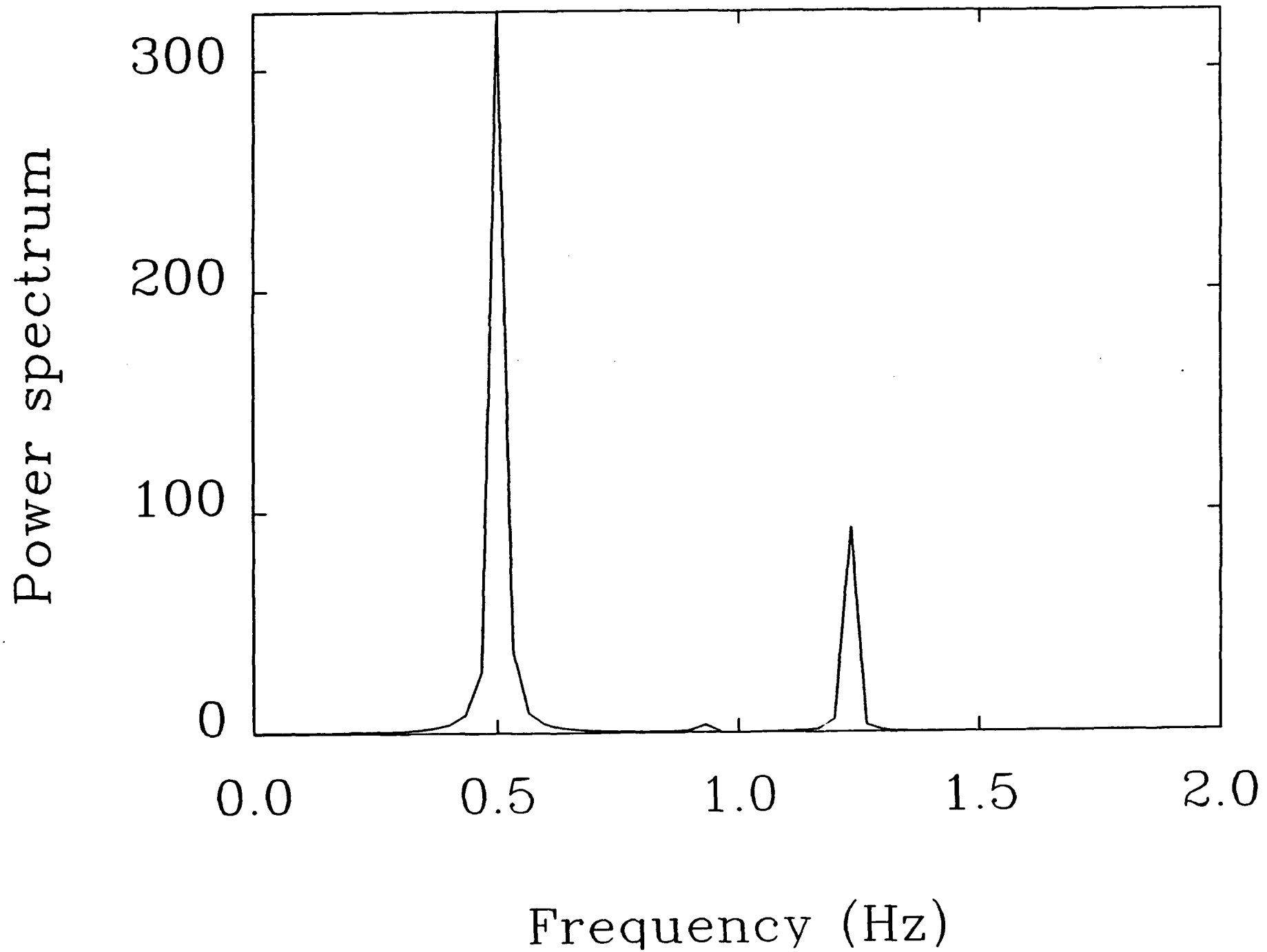

Figure 3b

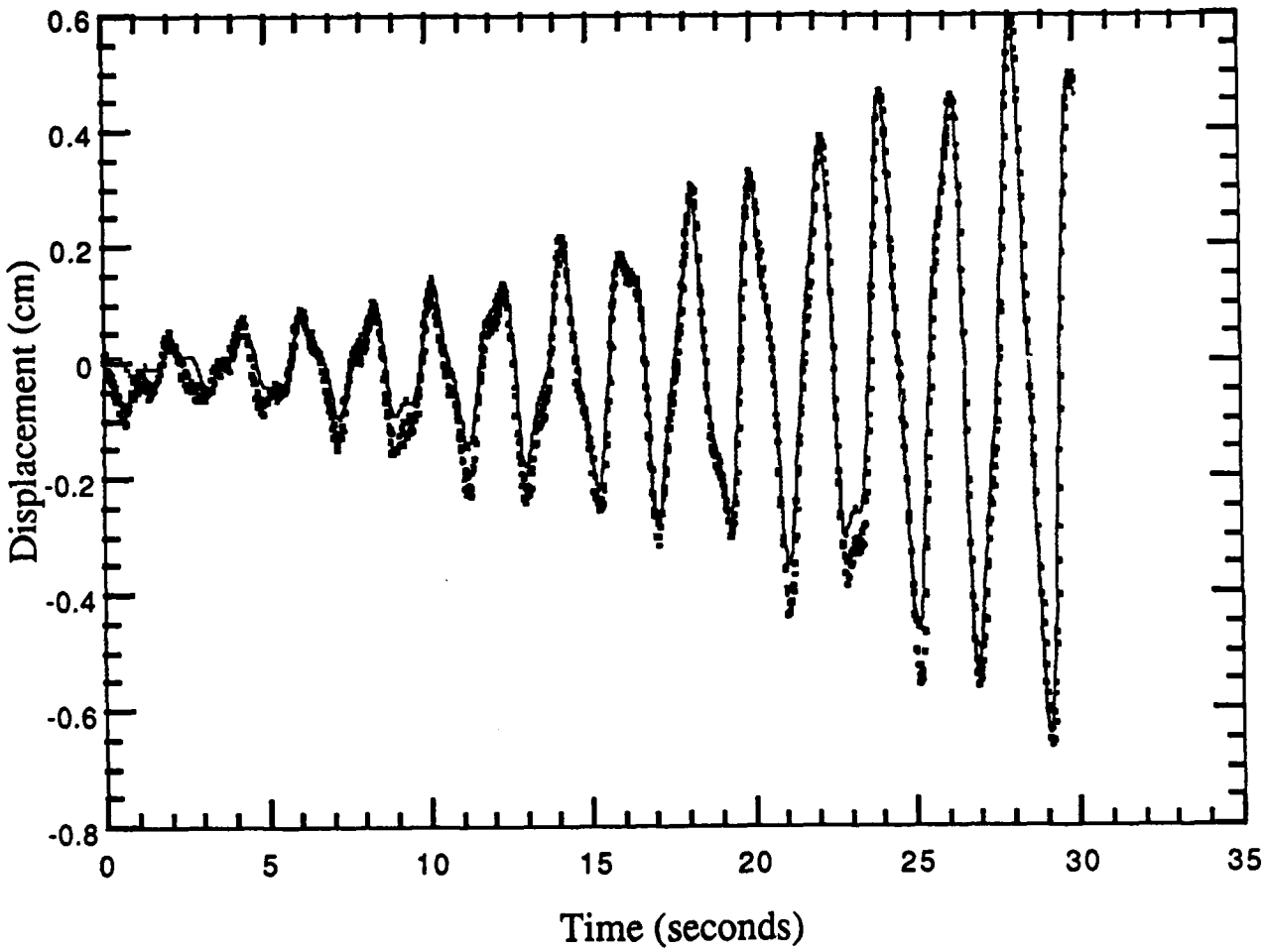
0.6
0.4
0.2
0
-0.2
-0.4
-0.6
-0.8
Displacement (cm)
0
5
10
15
20
25
30
35
Time (seconds)

Figure 3c

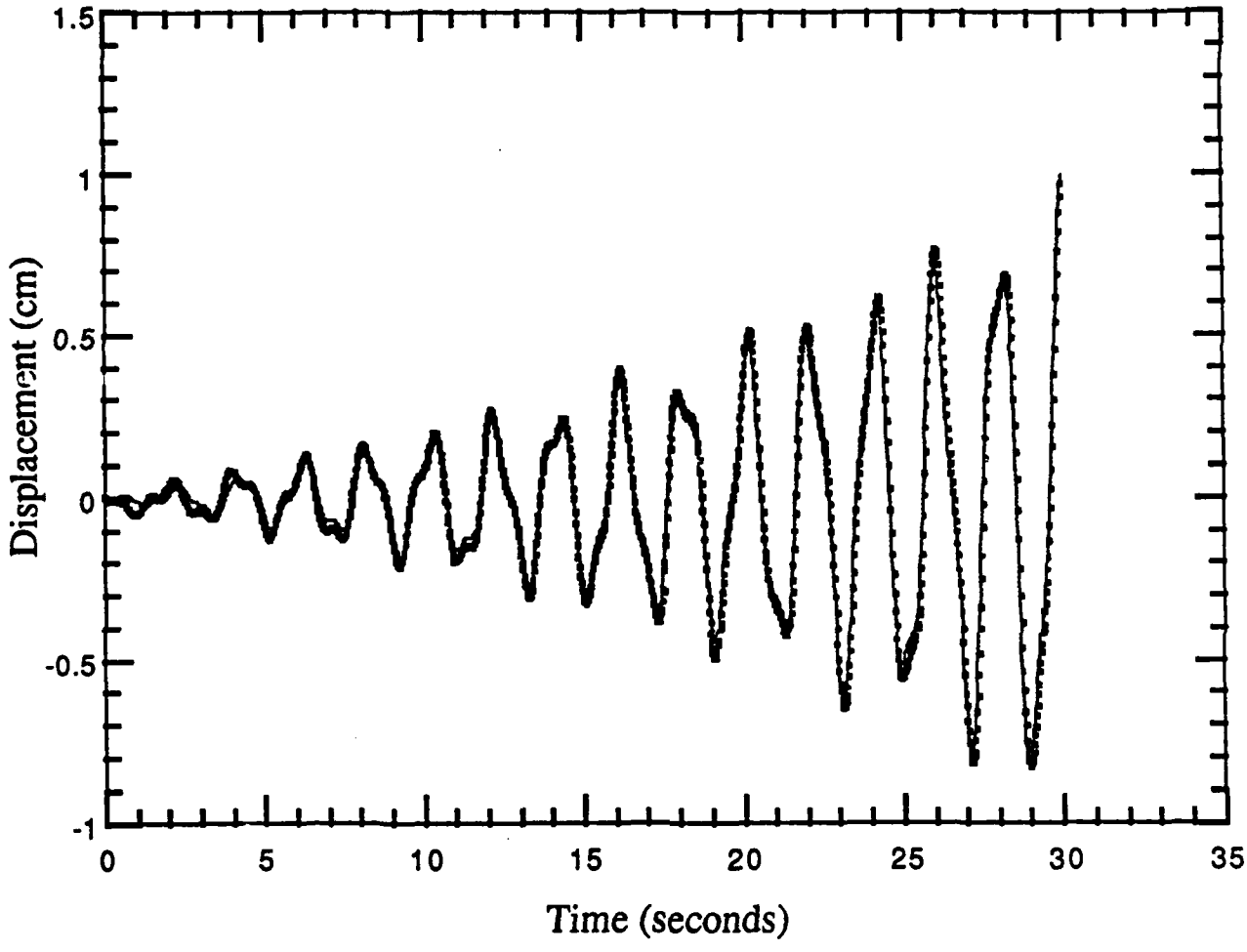

Figure 3d

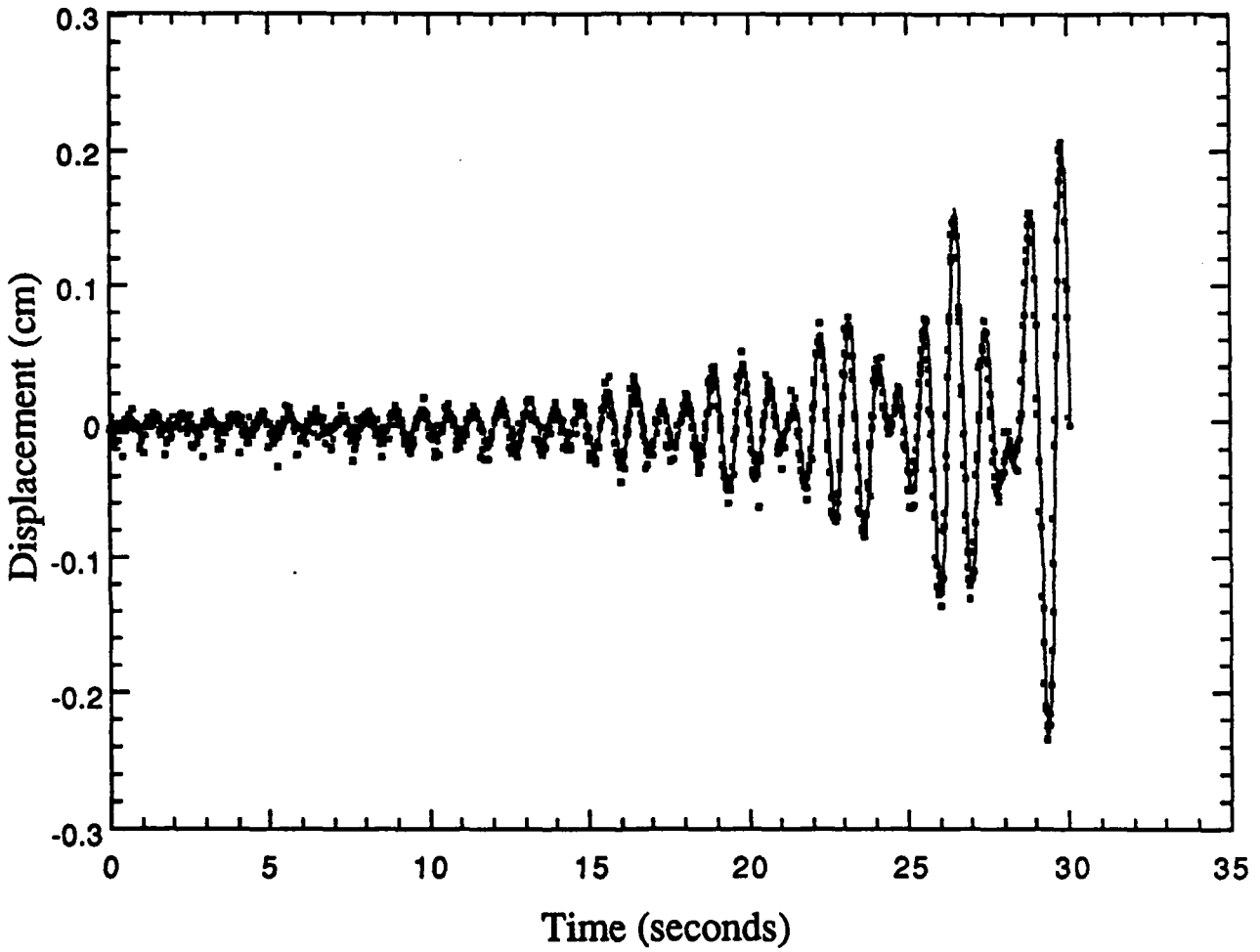
0.3
0.2
0.1
0
-0.1
-0.2
-0.3
Displacement (cm)
0
5
10
15
20
25
30
35
Time (seconds)

Figure 4a

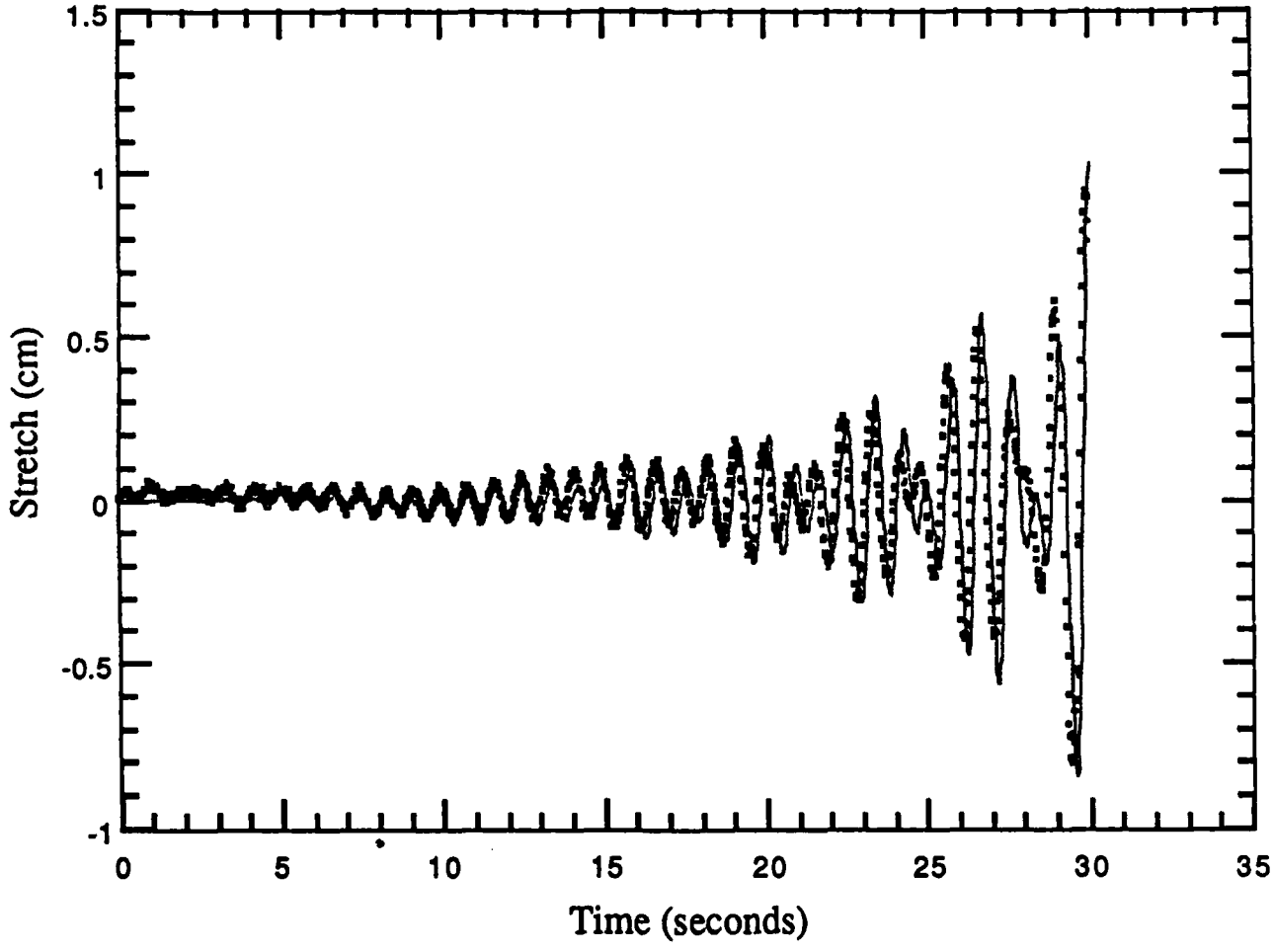

Figure 4b

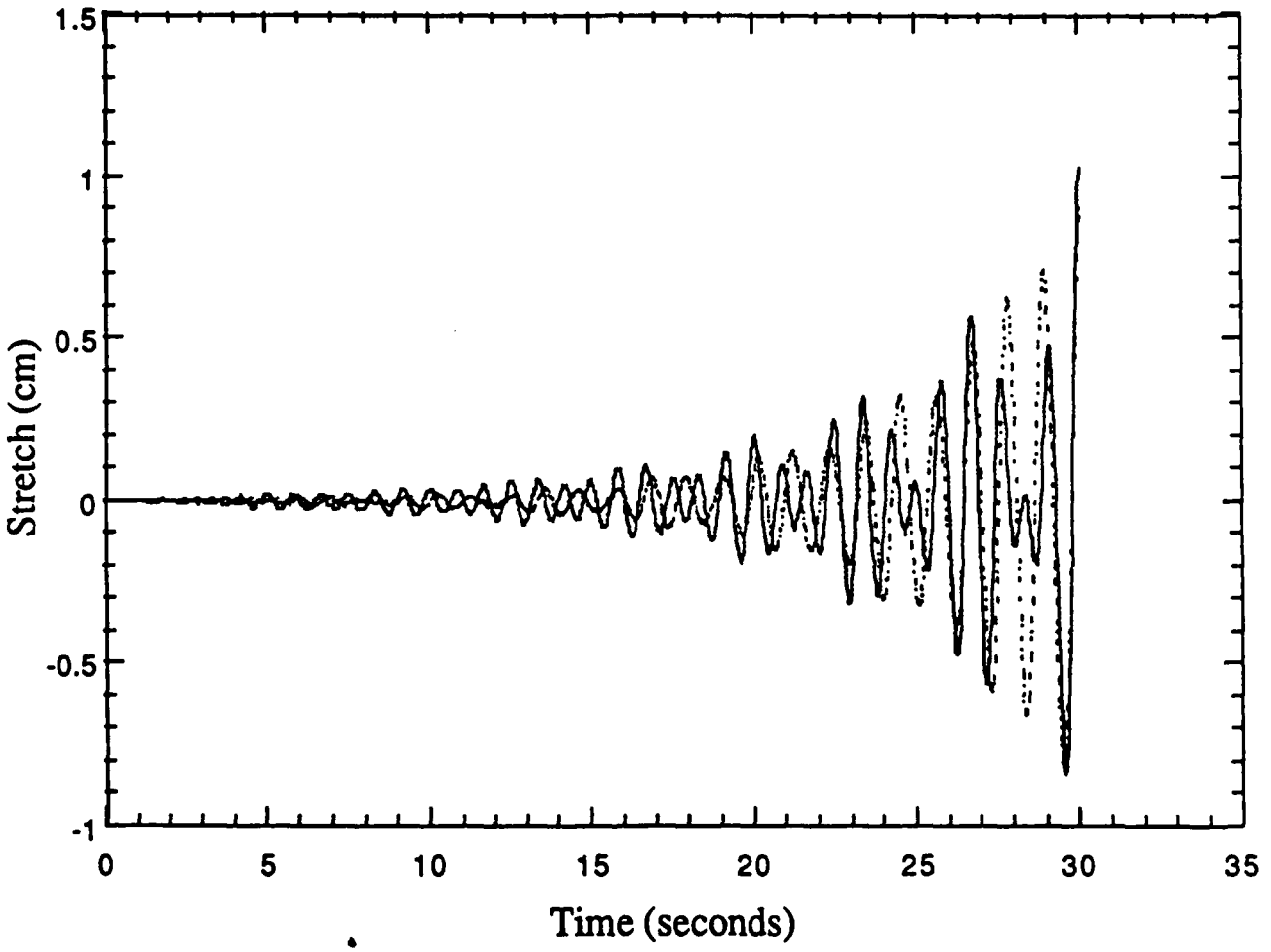

Figure 4c

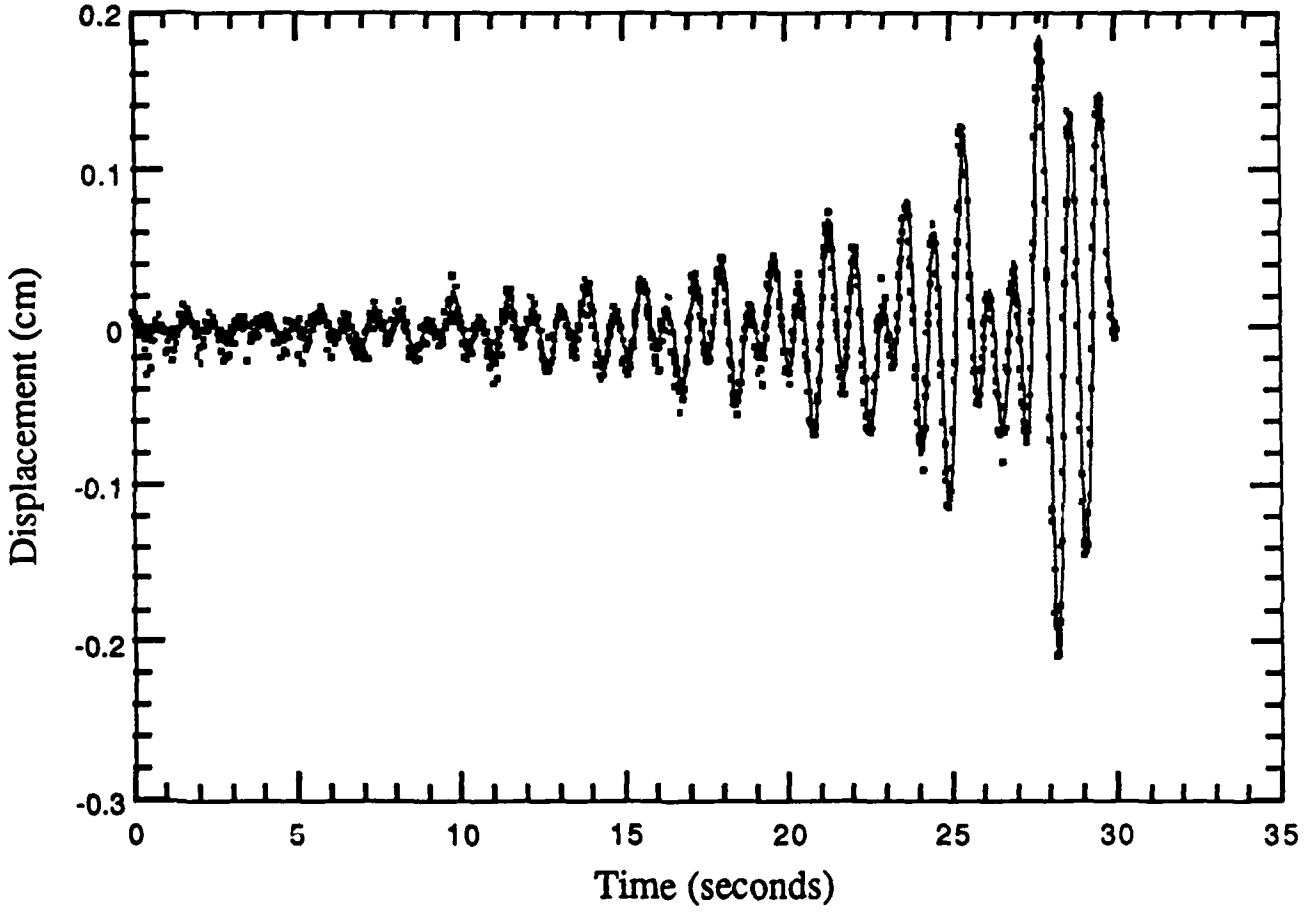
0.2
0.1
0
-0.1
-0.2
-0.3
Displacement (cm)
0
5
10
15
20
25
30
35
Time (seconds)

Figure 5a

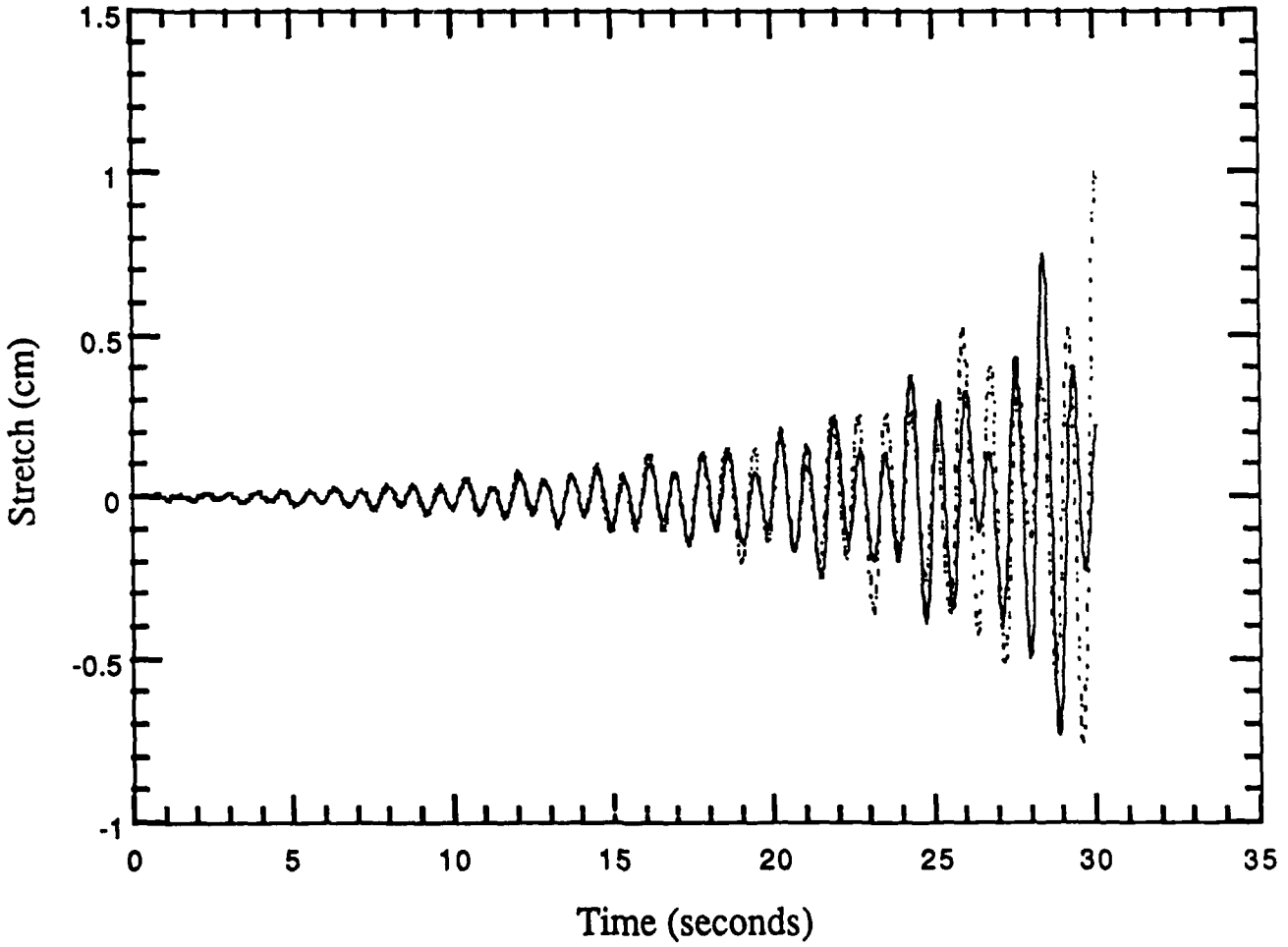

Figure 5b

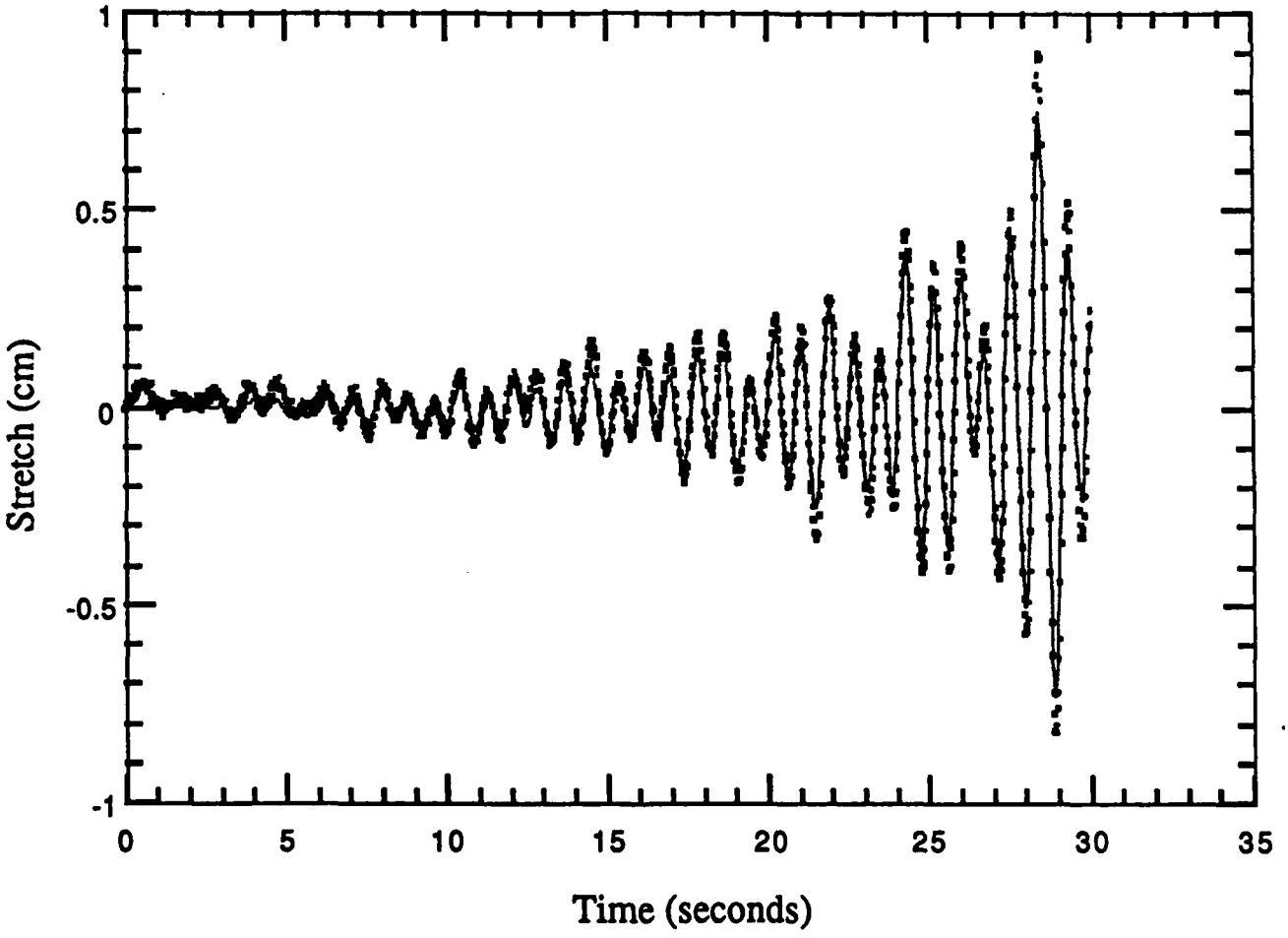

Figure 5c